## Remarks

Reconsideration and withdrawal of the rejections of the claims, in view of the amendments and remarks herein, is respectfully requested. Claims 53 and 73-74 are amended and claims 57, 77 and 80 are canceled. The amendments are intended to advance the application and are not intended to concede to the Examiner's position or to prejudice the prosecution of the claims prior to amendment, which claims are present in a continuation of the above-identified application. Claims 53-55, 58-64, 66-68, 70, 72-75, 78-79, and 81-82 are now pending in this application.

Claims 53-55, 57, 64, 70, and 72-73 were objected to as containing typographical error. Applicant has amended claim 53 to overcome this objection.

### *The 35 U.S.C. § 112 Rejections*

The Examiner rejected claims 53-55, 57, 64, 70, 72-75, and 81-82 under 35 U.S.C. § 112, first paragraph, as lacking a clear written description. This rejection, as it may be maintained with respect to the pending claims, is respectfully traversed.

With respect to the Examiner's assertion at page 4 of the Office Action regarding the structure of variant PBR genes, the Examiner is reminded that Applicant need not teach what is well-known to the art. The structure of PBR genes was known prior to Applicant's filing as evidenced by Riond et al. (Eur. J. Biochem., 195:305 (1991)) and Hardwick et al. (Proc. of the Am. Assoc. Can. Res., 38:233 (1997)) (a copy of each is enclosed herewith for the Examiner's convenience). Thus, the amendments to claims 53 and 74, and the cancellation of claim 57, obviate the § 112(1) written description rejection of claims 53-55, 57, 64, 70, and 72-75.

Although the Examiner rejected claims 81-82 as lacking an adequate written description "for the same reasons of record", none of the reasons listed on pages 3-4 of the Office Action apply to claims 81-82.

Therefore, withdrawal of the written description rejection of claims 53-55, 57, 64, 70, 72-75, and 81-82 under 35 U.S.C. § 112, first paragraph, is appropriate and respectfully requested.

The Examiner also rejected claims 53-55, 57, 64, 70, 72-75, 77-80, and 81-82 under 35 U.S.C. § 112, first paragraph, because the specification, while being enabled for a polynucleotide sequence consisting of SEQ ID NO:1 or 2, or a nucleic acid consisting of a polynucleotide

sequence encoding a polypeptide consisting of SEQ ID NO:3, allegedly lacks enablement for complements of SEQ ID NO:1 or 2 that inhibit cell proliferation, or of nucleic acids "comprising" a fragment of 7 to 40 nucleotides of SEQ ID NO:1 or 2, or a full length PBR gene encoding SEQ ID NO:2, or PBR gene encoding a PBR protein that "comprises" the mutant residues threonine 147 or arginine 162, or that "comprises" SEQ ID NO:3, or "a PBR gene". As this rejection may be maintained with respect to the pending claims, it is respectfully traversed.

The amendments to claims 53 and 74, and the cancellation of claims 57, 77 and 80, render the enablement rejection of claims 53-55, 57, 64, 70, 72-75, and 77-80 moot.

With regard to the enablement rejection of claims 81-82, the Examiner is requested to consider that the structure of a PBR gene was known (see above) and that the Examiner has conceded that the specification enables "a polynucleotide sequence consisting of SEQ ID NO:1 or 2" and "a nucleic acid consisting of a polynucleotide sequence encoding a polypeptide consisting of SEQ ID NO:3".

Accordingly, withdrawal of the § 112(1) enablement rejection is respectfully requested.

*The 35 U.S.C. § 102(e) Rejection*

The Examiner rejected claim 81 under 35 U.S.C. § 102(e) as being anticipated by Sorge et al. (U.S. Patent No. 5,663,062) or Studier (U.S. Patent No. 5,407,799). These rejections are respectfully traversed.

Claim 81 is directed to an isolated nucleic acid consisting of SEQ ID NO:1, SEQ ID NO:2, or the complement thereof. SEQ ID NO:1 and SEQ ID NO:2 each have 652 nucleotides.

U.S. Patent No. 5,663,062 discloses a library of oligonucleotides that are typically from about 5 to 10 nucleotides in length (abstract). The library is used to construct larger oligonucleotides of preselected sequence (column 4, lines 21-25), which are useful as primers for DNA sequencing and PCR (column 4, lines 18-20). Two types of libraries are disclosed, both of which employ oligonucleotides (column 5, lines 53-55).

U.S. Patent No. 5,401,799 discloses a method for high-volume sequencing of nucleic acid with random or directed priming with libraries of oligonucleotides (title).

Neither the '799 patent nor the '062 patent discloses an isolated nucleic acid consisting of SEQ ID NO:1, SEQ ID NO:2, or the complement thereof.

Accordingly, withdrawal of the § 102(e) rejections is respectfully requested.

## CONCLUSION

Applicant respectfully submits that the claims are in condition for allowance and notification to that effect is earnestly requested. The Examiner is invited to telephone Applicant's attorney (612) 373-6959 to facilitate prosecution of this application.

If necessary, please charge any additional fees or credit overpayment to Deposit Account No. 19-0743.

Respectfully submitted,

VASSILIOS PAPADOPOULOS ET AL.,

By their Representatives,

SCHWEGMAN, LUNDBERG, WOESSNER & KLUTH, P.A.
P.O. Box 2938
Minneapolis, MN 55402
(612) 373-6959

Date November 23, 2005 By _____
Janet E. Embretson
Reg. No. 39,665

CERTIFICATE UNDER 37 CFR 1.8: The undersigned hereby certifies that this correspondence is being deposited with the United States Postal Service with sufficient postage as first class mail, in an envelope addressed to: Mail Stop AF, Commissioner of Patents, P.O. Box 1450, Alexandria, VA 22313-1450, on this 23 day of November, 2005.

LISA POSORSKE _____

Name Signature

Eur. J. Biochem. 199, 305 – 311 (1991)

00142956910003 6H



# Molecular cloning and chromosomal localization of a human peripheral-type benzodiazepine receptor

Joelle RIOND[1], Marie Genevieve MATTEI[3], Mourad KAGHAD[2], Xavier DUMONT[2], Jean Claude GUILLEMOT[1], Gerard LE FUR[1], Daniel CAPUT[2] and Pascual FERRARA[1]

[1] Laboratoire de Biochimie des Protéines
[2] Laboratoire de Biologie Moléculaire, Sanofi Elf Bio-Recherches, Labège, France
[3] Unité 242, Institut National de la Recherche Médicale, Groupe Hospitalier de la Timone, Marseille, France

(Received June 29, 1990) – EJB 90 0761

The sequencing of endopeptidase-generated peptides from the peripheral binding site (PBS) for benzodiazepines, purified from a Chinese hamster ovary (CHO) cell line, produced internal sequence information, and confirmed and extended the $NH_2$-terminal PBS sequence that we previously reported. Since the sequences were highly similar to the corresponding rat PBS sequences, we investigated whether they were also conserved in human PBS. Scatchard analysis of [$^3$H]PK11195 (a derivative of isoquinoline carboxamide) binding and photoaffinity labeling with [$^3$H]PK14105 (a nitrophenyl derivative of PK11195) revealed that CHO PBS and human PBS are closely related. Furthermore a rabbit antiserum raised against three peptides synthesized on the basis of the CHO PBS sequence immunoprecipitate the solubilized U937 PBS and also recognize the human protein in an immunoblot analysis. Based on these results, we screened a U937 cell cDNA library with four oligonucleotide probes derived from the CHO sequence. Two of the probes hybridized with several clones that we isolated and sequenced. One of these, h-pPBS11, is 831 nucleotides and contains a full-length representation of human PBS mRNA. The amino acid sequence of human PBS deduced from the cDNA is 79% identical to that reported for rat PBS, however, human PBS contains two cysteines while rat PBS is characterized by the absence of this amino acid. Using the cDNA of human PBS as a probe, the PBS gene was located in the 22q13.3 band of the human genome.

Benzodiazepines are psychoactive drugs with sedative, anxiolytic and anticonvulsant properties. They exert these actions through receptors located in the central nervous system [1, 2]; however some benzodiazepines also interact with a different type of receptor present mainly in the mitochondrial compartment of peripheral tissues [3 – 5]. The physiological role of this peripheral-type receptor is still unclear, although several studies have shown that peripheral-type benzodiazepine ligands can induce monocyte chemotaxis [6], cell differentiation [7 – 10] and steroidogenesis [11 – 13] *in vitro*.

Recently a cDNA coding for the rat peripheral-type benzodiazepine receptor (PBS) was isolated. The deduced amino acid sequence corresponds to a protein of 169 amino acids, with five putative transmembrane regions, and without a typical mitochondrial-targeting sequence [14]. The sequence following the first methionine in the open reading frame is highly similar to the $NH_2$-terminal sequence of a CHO PBS that we previously reported [15].

We present here the sequences of endopeptidase-generated peptides from purified CHO PBS. Some of these peptide sequences, identical to that from rat PBS, were also conserved in human PBS present in the histiocytic lymphoma cell line U937; this cell line was chosen as a human model because monocyte/macrophage chemotaxis is a well-documented physiological role of PBS ligands [6]. Based on the peptide sequences, we constructed four mixed-sequence oligonucleotide probes that were used to isolate a full-length cDNA clone coding for human PBS from a cDNA library constructed from the U937 cell line. Finally, using the cDNA of human PBS as a probe, the PBS gene was located in the q13.3 region of the long arm of chromosome 22 by *in situ* hybridization.

## MATERIALS AND METHODS

### *Cell lines and culture*

The CHO cells [16] were cultured and collected as described [17]. The human U937 cell line [18] was grown in suspension in RPMI 1640 medium containing 10% heat-inactivated fetal calf serum, 2.5 mM sodium pyruvate, 5 mM Hepes, 4 mM glutamine, 100 IU/ml penicillin and 50 µg/ml streptomycin.

*Correspondence to* D. Caput, Sanofi Elf Bio-Recherches, Boîte Postale 137, F-31328 Labège Cédex, France

*Abbreviations*. PBS, peripheral binding site; CHO, Chinese hamster ovary.

*Enzyme*. *Staphylococcus aureus* V8 protease (EC 3.4.21.19).

*Note*. The novel nucleotide sequence data published here has been deposited with the EMBL sequence data bank and is available under accession number M36035

*[$^3$H]PK11195 binding and [$^3$H]PK14105 photolabeling of CHO and U937 cell lines*

Saturation experiments of CHO and U937 PBS with [$^3$H]PK11195 (66.0 Ci/mmol, CEA, Gif-sur-Yvette, France) were performed as previously described [15]. Photolabeling experiments were performed on 0.5 ml of either a cell suspension ($2 \times 10^6$ cells/ml), or a mitochondrial suspension (2 mg protein/ml) with [$^3$H]PK14105 (87.0 Ci/mmol, CEA, Gif-sur-Yvette, France) as described [15]. The photolabeled samples were either directly analysed by SDS/PAGE or extensively washed and used for the immunoprecipitation experiments.

*Peptide preparation and sequencing*

For peptide preparation, approximately $10^6$ dpm [$^3$H]-PK14105-photolabeled CHO PBS were added to CHO cell mitochondria, and CHO PBS was purified as previously described [15], except that the final HPLC step was replaced by SDS/PAGE. The PBS band of the unfixed gel was excised and digested *in situ* with *Staphylococcus aureus* V8 protease (Sigma) according to a modification of the method described by Cleveland et al. [19]; the peptides generated were concentrated into a thin band at the migration front of a stacking gel instead of being separated in a classical discontinuous SDS/PAGE. The peptide-containing band was then excised, cut into small pieces and extracted overnight at 4°C in 100 µl 100 mM Tris buffer, pH 6.8, and 0.1% SDS. After centrifugation, the supernatant was directly loaded onto a reverse-phase HPLC column ($C_8$, 0.2 cm × 10 cm, Brownlee) and eluted for 15 min with a 1–70% linear gradient of acetonitrile containing 0.1% trifluoroacetic acid at a flow rate of 0.3 ml/min. Elution was monitored at 216 nm and peaks were collected manually. 10% of each peak was used for measuring radioactivity by liquid-scintillation counting and the rest was used for sequence determination. The $NH_2$-terminal sequence analysis was performed as previously described [15] using a gas-phase sequenator (Applied Biosystems).

*Peptide synthesis and immunization*

Three peptides were simultaneously synthesized on methylbenzylhydroxylamine resin [20]. SP1 corresponded to sequence 1–15 of P4 (APSWVPAVGLTLAPSXGGFMXAYFV). SP2 corresponded to positions 1–20 of peptide P4 with a glycine in the undetermined position 16. SP3 corresponded to positions 1–21 of P5 (LGGFTEEAVVPLGLYTGQLALNWAWPPIF), with a leucine in position 1 replaced by aspartic acid. The three peptides contained a cysteine at the COOH-terminus. The synthetic peptides were characterized by amino acid analysis and complete sequencing. A mixture of the three peptides (0.5 mg each) was injected into rabbits subcutaneously every ten days. Antisera were titrated by ELISA using the synthetic peptides as coating antigen.

*Immunoblot analysis*

Cell homogenates were solubilized in sample buffer, separated on SDS/PAGE (15%), and transferred on to a nitrocellulose membrane in a semi-dry transfer apparatus (LKB). The membrane was then saturated in 3% bovine serum albumin and incubated with anti-peptide antiserum at a dilution factor of 1/500. The complexes were revealed by autoradiography of the dry sheet after incubation with $^{125}$I-labeled protein A (New England Nuclear).

*Immunoprecipitation*

A freshly photolabeled CHO or U937 cell mitochondrial preparation was solubilized in 50 mM Tris buffer, pH 8.0, 150 mM NaCl, 1% Nonidet P40, 0.1% SDS and 0.5% sodium deoxycholate, at a final protein concentration of 1 mg/ml. After 60 min at 4°C, the mixture was centrifugated for 30 min at 10000 × *g* and the supernatant collected. For each assay, 5 µl supernatant (approximately 10000 dpm) were diluted tenfold in solubilization buffer containing 0.1% bovine serum albumin and mixed with anti-peptide antiserum (1/100). After incubation overnight at 4°C, 50 µl activated Pansorbin (Calbiochem) were added and incubated for 3 h. The Pansorbin was then pelleted, washed with water and heated for 10 min at 80°C in electrophoresis sample buffer. An aliquot of supernatant was used for measuring radioactivity, the rest was resolved by SDS/PAGE and revealed by autoradiography.

*cDNA cloning*

Poly(A)-rich RNA was prepared from the human cell line U937 according to Cathala et al. [21]. A cDNA library was constructed using a pTZ19 vector according to Caput et al. [22], and contained approximately $10^6$ recombinant bacteria. Four synthetic oligonucleotides, (1) 5′-(CAC GGC GGG T/CAC CCA GGA)-3′, (2) 5′-(CAG AGT C/GAG GCC CAC GGC)-3′, (3) 5′-(CTC CTC TGT GAA G/ACC G/TCC)-3′, and (4) 5′-(GAA GAT GGG GGG CCA TGC)3′, were derived from different parts of the sequenced peptides and used as probes to screen the library by *in situ* colony hybridization.

*DNA sequence analysis*

The DNA sequencing was performed by the dideoxy-chain-termination method [23] using restriction fragments cloned in M13 mp18 and M13 mp19 (Pharmacia).

*Gene mapping by* in situ *hybridization. In situ* hybridization was carried out on chromosome preparations obtained from phytohemagglutinin-stimulated human lymphocytes cultured for 72 h. 5-Bromodeoxyuridine was added for the final 7 h of culture (60 µg/ml medium) to ensure a posthybridization chromosomal banding of good quality. For the probe preparation the p-hPBS11 clone, containing an 840-base insert was $^3$H-labeled by nick translation to a specific activity of $1.7 \times 10^6$ dpm/µg. The radiolabeled probe was hybridized to metaphase spreads at a final concentration of 100 ng/ml hybridization solution [24]. After coating with nuclear track emulsion (KODAK NTB2), the slides were exposed for 12 days at 4°C, then developed. To avoid any slipping of silver grains during the banding procedure, chromosome spreads were first stained with buffered Giemsa solution and photographed at metaphase. R banding was then performed by the fluorochrome/photolysis/Giemsa method and rephotographed at metaphase before analysis.

## RESULTS

*Purification and sequencing of CHO PBS peptides*

The CHO PBS was solubilized and purified from [$^3$H]PK14105-photolabeled mitochondria as described previously [15]. Minor contaminating polypeptides present after the final HPLC step were completely resolved from PBS by purification on SDS/PAGE. The PBS band (approximately 200 pmol) was excised from the unfixed SDS/PAGE and di-

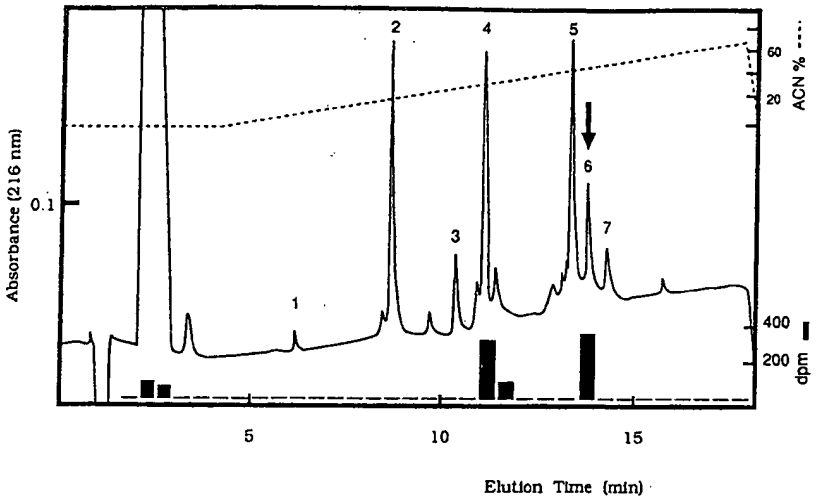


Fig. 1. *Elution pattern of endopeptidase-generated peptides from CHO PBS.* Approximately 200 pmol purified PBS digested with *S. aureus* V8 protease was loaded on to a $C_8$ reverse-phase HPLC column and eluted with a 1–70% linear gradient of acetonitrile containing 0.1% trifluoroacetic acid in 15 min at a flow rate of 0.3 ml/min. Elution was monitored at 216 nm and peaks were manually collected. 10% of each peak was used for measuring radioactivity and the rest was used for sequence determination. The arrow indicates the elution position of the intact PBS

gested *in situ* with *S. aureus* V8 protease. The resulting peptides were eluted from the gel and finally separated by narrow-bore reverse-phase HPLC (Fig. 1). The most prominent of these peptides (1–7) were subjected to sequence analysis. Unambiguous sequence information was obtained from three peptides: P4 (see above), P5 (see above) and P6 (APXWVPAVGLTLAP). The initial yields of peptides P4, P5 and P6 were 13, 30 and 5 pmol, respectively. Two of the sequences obtained, P4 and P6, confirmed and extended the previously determined $NH_2$-terminal sequence of intact PBS [15]. Radioactive determination of the fractions eluting from the HPLC revealed that almost all the loaded radioactivity from the covalently attached [$^3$H]PK14105 probe was recovered in peaks P4 and P6.

*Comparison of CHO and human PBS*

The specific binding of the isoquinoline carboxamide derivative [$^3$H]PK11195, a selective ligand for PBS, to a crude mitochondrial preparation from either CHO or U937 cells, was saturable (Fig. 2A and B). Linear-regression analysis of the Scatchard plots showed, in both cases, a single-component site with $K_d$ values of 4.8 nM and 9.8 nM for CHO and human PBS, respectively (Fig. 2A and B, insets). It should be noted, however, that the amount of PBS in CHO cells (1.1 pmol/$10^6$ cells) is tenfold higher than that in U937 cells (0.1 pmol/$10^6$ cells). To probe for homology, we used an antiserum raised against a mixture of three synthetic peptides corresponding to the sequences obtained from CHO PBS. This antiserum was able to immunoprecipitate a CHO and U937 mitochondrial 17-kDa protein specifically labeled with the photoaffinity probe [$^3$H]PK14105, a nitrophenyl derivative of PK11195 [25] (Fig. 2C). In both cases, the immunoprecipitation is inhibited by an excess of the synthetic peptides used for the preparation of the antiserum. This antiserum also recognized the 17-kDa protein in immunoblot analysis of total cell homogenates from both CHO and U937 cells (Fig. 2D).

*Isolation and analysis of human PBS cDNA*

A plasmid cDNA library was constructed from the U937 cell line. cDNA clones were isolated by hybridization with four synthetic oligonucleotides (see Materials and Methods). Only oligonucleotides 3 and 4 were able to hybridize to the same clones. The clones hybridizing with probes 3 and 4 were size selected. The largest of these clones, designated h-pPBS11 was sequenced. The nucleotide and predicted amino acid sequence of human PBS cDNA with 61 nucleotides of 5′-flanking and 260 nucleotides of 3′-flanking sequence are shown in Fig. 3. Total (probe 4) or partial (probes 1, 2 and 3) similarities with the four probes are found in h-pPBS11. Both the primary structure and the Northern blot analysis (results not shown) suggest that h-pPBS11 contains a full-length representation of the pBDZ-R mRNA. The amino acid sequences of human and rat PBS, as deduced from their respective cDNA, show an overall similarity of 79% (134 out of 169 amino acids) with 21 mutations in the $NH_2$-terminal half of the molecule and 14 in the COOH-terminal half (Fig. 4). The longest region of identity between the two molecules is located in the middle of the sequence where a stretch of 33 consecutive identical residues, Val80–Leu112, is found. Interestingly, while rat PBS does not contain cysteine, human PBS has two, one near the $NH_2$-terminus (position 19) and the other near the COOH-terminus end (position 153). The sequences of the CHO PBS peptides are also highly conserved when compared with the deduced human PBS sequence; 71% identity for P4 and 93% for P5 (Fig. 4).

*Chromosomal localization of human PBS*

The cDNA of human PBS was used as a probe for the chromosomal localization of the PBS gene (Fig. 5A). In the 150 metaphase cells examined after *in situ* hybridization, 286 silver grains were associated with the chromosomes, and 42 of these (14.7%) were located on chromosome 22; the distribution of grains in this chromosome was not random: 92.8% mapped to the q13.1-q13.3 region of the long arm of

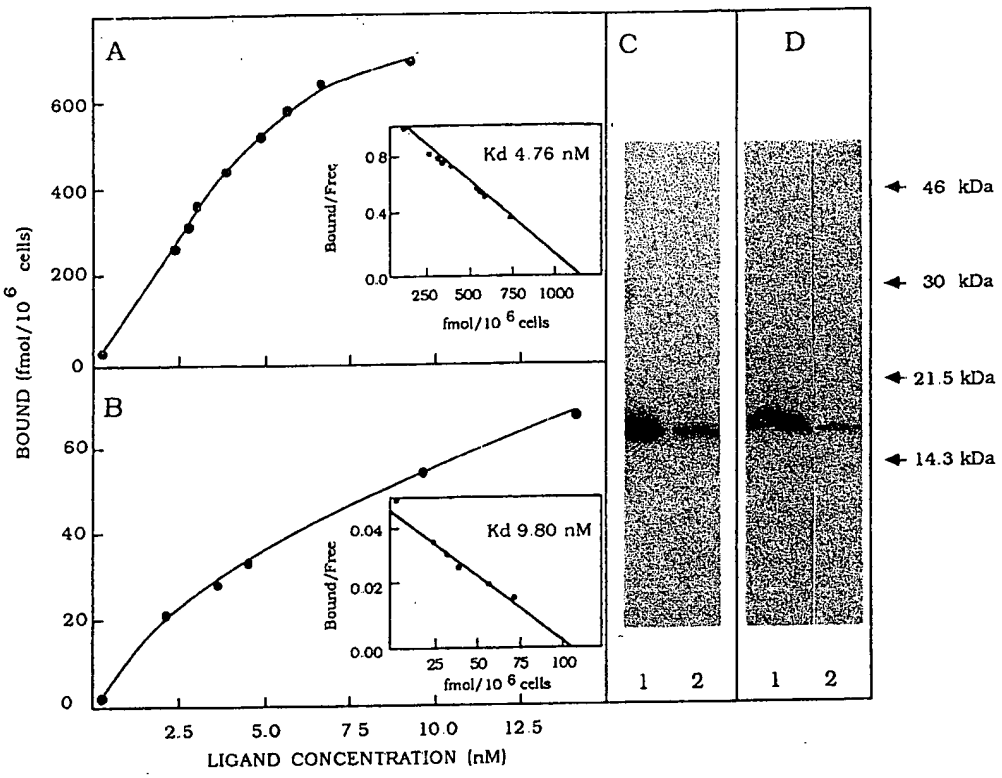


Fig. 2. *Comparison of CHO and U937 PBS.* Saturation and Scatchard plot of [$^3$H]PK11195 binding to total cell homogenates of (A) CHO and (B) U937 cells. (C) Autoradiograms of SDS/PAGE analysis of [$^3$H]PK14105-photolabeled CHO (lane 1) and U937 (lane 2) mitochondrial fraction solubilized and immunoprecipitated with the anti-(CHO peptide) antiserum. (D) immunoblot analysis of CHO (lane 1) and U937 (lane 2) total cell homogenates

```
-61 AGTGCCCTTCCCGGAGCGTGCCCTCGCCGCT GAGCTCCCCTGAACAGCAGCTGCAGCAGCC

  1 ATGGCCCCGCCCTGGGTGCCCGCCATGGGC TTCACGCTGGCGCCCAGCCTGGGGTGCTTC
    MetAlaProProTrpValProAlaMetGly PheThrLeuAlaProSerLeuGlyCysPhe

 61 GTGGGCTCCCGCTTTGTCCACGGCGAGGGT CTCCGCTGGTACGCCGGCCTGCAGAAGCCC
    ValGlySerArgPheValHisGlyGluGly LeuArgTrpTyrAlaGlyLeuGlnLysPro

121 TCGTGGCACCCGCCCCACTGGGTGCTGGGC CCTGTCTGGGGCACGCTCTACTCAGCCATG
    SerTrpHisProProHisTrpValLeuGly ProValTrpGlyThrLeuTyrSerAlaMet

181 GGGTACGGCTCCTACCTGGTCTGGAAAGAG CTGGGAGGCTTCACAGAGAAGGCTGTGGTT
    GlyTyrGlySerTyrLeuValTrpLysGlu LeuGlyGlyPheThrGluLysAlaValVal

241 CCCCTGGGCCTCTACACTGGGCAGCTGGCC CTGAACTGGGCATGGCCCCCCATCTTCTTT
    ProLeuGlyLeuTyrThrGlyGlnLeuAla LeuAsnTrpAlaTrpProProIlePhePhe

301 GGTGCCCGACAAATGGGCTGGGCCTTGGTG GATCTCCTGCTGGTCAGTGGGGCGGCGGCN
    GlyAlaArgGlnMetGlyTrpAlaLeuVal AspLeuLeuLeuValSerGlyAlaAlaAla

361 GCCACTACCGTGGCCTGGTACCAGGTGAGC CCGCTGGCCGCCCGCCTGCTCTACCCCTAC
    AlaThrThrValAlaTrpTyrGlnValSer ProLeuAlaAlaArgLeuLeuTyrProTyr

421 CTGGCCTGGCTGGCCTTCGCGACCACACTC AACTACTGCGTATGGCGGGACAACCATGGC
    LeuAlaTrpLeuAlaPheAlaThrThrLeu AsnTyrCysValTrpArgAspAsnHisGly

481 TGGCATGGGGGACGGCGGCTGCCAGAGTGA GTGCCCGGCCCACCAGGGACTGCAGCTGCA
    TrpHisGlyGlyArgArgLeuProGluEnd

541 CCAGCAGGTGCCATCACGCTTGTGATGTGG TGGCCGTCACGCTTTCATGACCACTGGGCC
601 TGCTAGTCTGTCAGGGCCTTGGCCCAGGGG TCAGCAGAGCTTCAGAGGTTGCCCCACCTG
661 AGCCCCCACCCGGGAGCAGTGTCCTGTGCT TTCTGCATGCTTAGAGCATGTTCTTGGAAC
721 ATGGAATTTTATAAGCTGAATAAAGTTTTT GACTTCCTTTAAAAAAAAAA...
```

Fig. 3. *cDNA sequence and derived amino acid sequence of human PBS.* The sequences corresponding to the oligonucleotide probes used to screen the U937-derived cDNA library are underlined

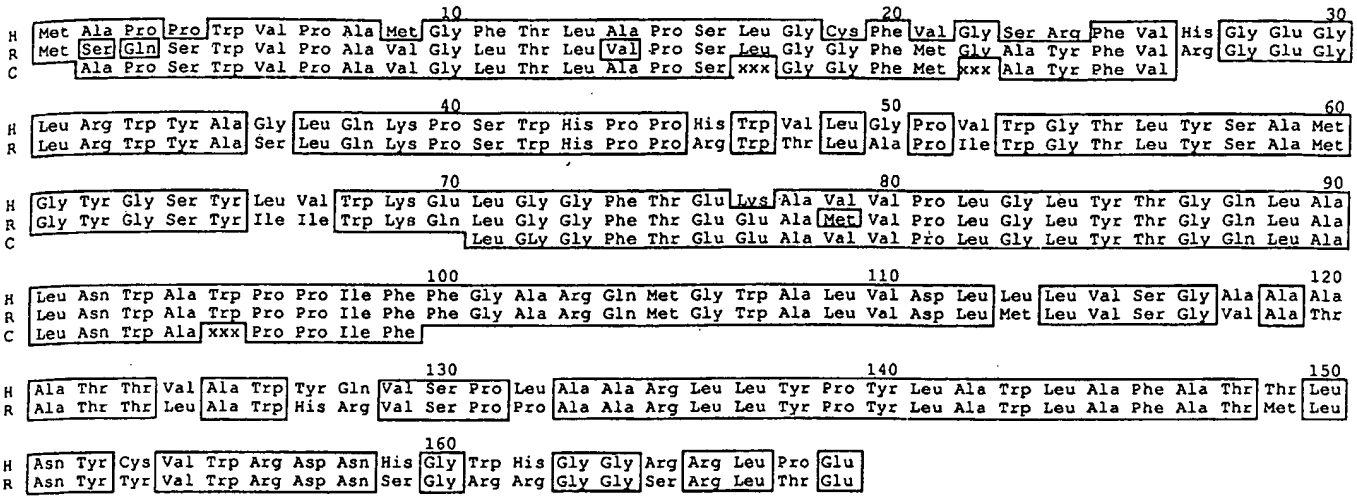


Fig. 4. *Comparison of the amino acid sequences of the human (h), rat (r) and CHO (c) PBS.* Identical amino acids are boxed

chromosome 22, with a maximum in the q13.3 band (Fig. 5B). These results allowed mapping of the p-hPBS11 probe to the 22 q13.3 band of the human genome.

## DISCUSSION

We recently purified and partially characterized a 17-kDa PBS present in the mitochondria of the CHO cells [15]. The amino acid composition and the $NH_2$-terminal sequence of the CHO PBS protein showed that it is closely related to the rat 17-kDa PBS protein recently cloned [14]. Attempts to obtain internal amino acid sequence information after enzymatic digestion of purified CHO PBS in solution resulted in a very low recovery of the generated peptides. Since these problems were probably due to the hydrophobic nature of the protein, we decided to perform an enzymatic digestion with the *S. aureus* V8 protease *in situ*, then to extract the resulting peptides from the gel, and to separate them by reverse-phase HPLC. This procedure allowed us to obtain several purified peptides that, after analysis, confirmed and extended the $NH_2$-terminal sequence already determined and produced additional sequence information. Furthermore, the presence of radioactivity from the photoaffinity probe, [$^3$H]PK14105, associated with the peptides, corresponding to the described $NH_2$-terminal sequences, supported the assignment of this sequence as part of PBS.

Since the peptide sequences of CHO PBS are highly similar to the corresponding sequences of rat PBS deduced by cDNA cloning, we decided to determine whether these sequences were also conserved in human PBS, to use this information for cloning the human molecule. The histiocytic lymphoma cell line U937 was used as a source of human PBS since monocyte/macrophage chemotaxis is a well-documented physiological role of PBS ligands [6]. Scatchard analysis of [$^3$H]PK11195 binding, photoaffinity labeling with [$^3$H]-PK14105 and an immunological comparison revealed that CHO PBS and human PBS were closely related. Furthermore, the pharmacological properties of CHO and U937 PBS, evaluated in displacement experiments of [$^3$H]PK11195 by PK11195, Ro5-4864, diazepam and clonazepam, were similar (results not shown). Based on these results, we screened a U937-cell-derived cDNA library with four oligonucleotide probes derived from the CHO sequences. Two of the probes hybridized with several clones which we isolated and sequenced. One of these, h-pPBS11, is 831 nucleotides, and contains a full-length representation of human PBS mRNA. The deduced amino acid sequence of human PBS is 79% identical to that reported for rat PBS and, when compared with the determined sequence of CHO PBS, the identity is 71% for P4 and 93% for P5. The determined $NH_2$-terminal sequence of CHO PBS is almost identical to the human sequence following the initial methionine, but whether or not the $NH_2$-terminal residue is modified, as suggested for rat [14] and CHO [15] PBS, is not known. Human PBS, as with rat PBS, does not contain a typical mitochondrial-targeting sequence.

Although closely related, human and rat PBS show several sequence differences which explain the different affinity that some peripheral ligands have for human and rat PBS. For example, Ro5-4864 binds with much higher affinity to rat PBS than to human PBS [26]. Interestingly, it has also been reported that 6-thioguanine causes inhibition of Ro5-4864 binding to human PBS, and that this inhibition was reversed by the presence of 2-mercaptoethanol, suggesting the formation of a mixed disulfide between the 6-thiopurine and a PBS thiol [10]. Although rat PBS is characterized by the absence of cysteine, human PBS contains two: one near the $NH_2$-terminus (position 19) and the other near the COOH-terminus (position 153). Of the two cysteines, the one in position 19 seems more likely to be involved, directly or indirectly, in the binding site, since radioactivity from the photoaffinity probe [$^3$H]PK14105 is covalently linked to the peptides corresponding to the $NH_2$-terminal sequence of the protein. It should be noted, too, that this cysteine is in the $NH_2$-terminal 25 amino acids, where differences predominate. Using the cDNA of human PBS as a probe, we located the PBS gene in the 22q13.3 band of the human genome. Chromosome 22 is involved in a relative high number of inherited and acquired diseases, in particular malignancies. The availability of this new cloned probe for the distal region of the long arm of chromosome 22 may help to characterize some of the DNA defects involved in those diseases [27]. Among other genes located on the long arm of chromosome 22 are mitochondrial aconitase 2 (*ACO2*), cytochrome *b*-5 reductase (*DIA1*), arylsulfatase A (*ARSA*) and platelet-derived growth factor $\beta$ polypeptide (*PDGF$\beta$*) [28].

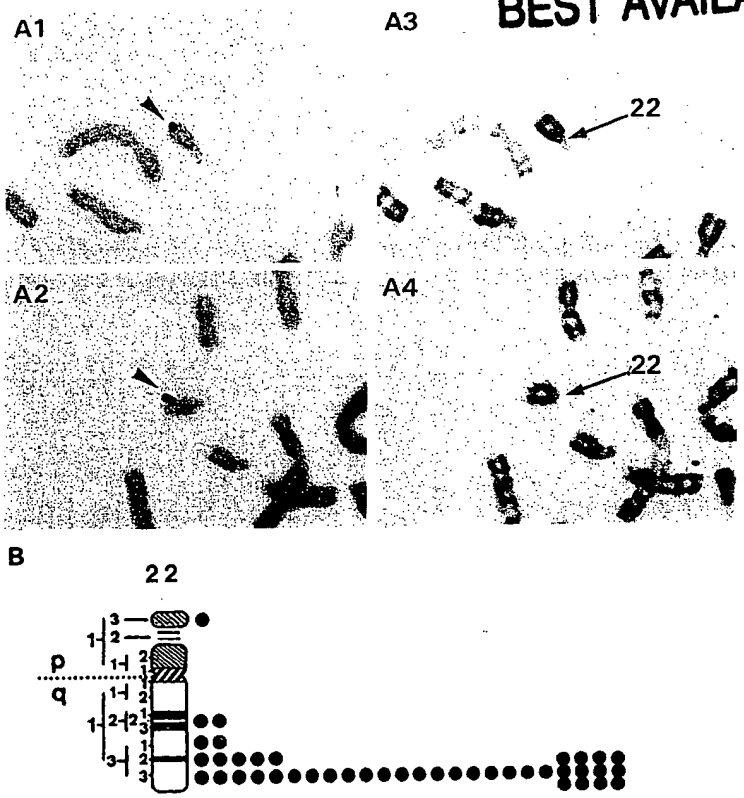


Fig. 5. *Chromosomal localization of human PBS.* (A1 and A2) Two partial human metaphases showing the specific site of hybridization to chromosome 22. Arrowheads indicate silver grains on Giemsa-stained chromosomes after autoradiography. (A3 and A4) Chromosomes with silver grains identified by R-banding as described in Materials and Methods. (B) Idiogram of the human G-banded chromosome 22 illustrating the distribution of labeled sites for the human PBS probe

The transfection experiments performed by Sprengel et al. [14] indicated that this 17-kDa protein is sufficient for the binding of PBS ligands. However, previous reports indicated that other proteins with molecular mass in the range 30–35 kDa are specifically either photolabeled with flunitrazepam [29] or acylated with AHN086 [30]. Whether or not the proteins labeled by these two ligands are the same is not known. Radiation inactivating experiments suggested a molecular mass of 34 kDa for PBS [31], and a molecular mass of 23 kDa for the isoquinoline-carboxamide-binding site [32]. Interestingly, we reported that a 33-kDa protein, in addition to the 17-kDa protein, can also be labeled with [$^3$H]PK14105 [15]. Taken together, these results strongly suggest that proteins other than the PBS 17-kDa protein can interact specifically either with benzodiazepines or with isoquinoline carboxamide derivatives. Whether or not these proteins are part of a single functional peripheral-type benzodiazepine receptor is not known. The existence of different peripheral-type benzodiazepine receptors cannot be excluded, and work is in progress in our laboratory to characterize other molecules which may help to answer some of these questions.

We thank C. Cassan, J. Capdevielle, B. Delpech and P. Chalon for excellent assistance. N. Vita, E. Marchese, A. Minty, and J. Hanoune for useful discussions. B. Beutler for critical reading of the manuscript.

## REFERENCES

1. Mohler, H. & Okada, T. (1977) *Science 198*, 849–851.
2. Squires, R. F. & Braestrup, C. (1977) *Nature 269*, 702–704.
3. Braestrup, C. & Squires, R. F. (1979) *Eur. J. Pharmacol. 48*, 263–270.
4. Anholt, R. R. H., De Souza, E. B., Oster-Granite, M. L. & Snyder, S. H. (1985) *J. Pharmacol. Exp. Ther. 233*, 517–526.
5. De Souza, E. B., Anholt, R. R. H., Murphy, K. M. M., Snyder, S. H. & Kuhat, M. J. (1985) *Endocrinology 116*, 567–573.
6. Ruff, M. R., Pert, C. B., Weber, R. J., Wahl, L. M., Wahl, S. M. & Paul, S. M. (1985) *Science 229*, 1281–1283.
7. Clarke, G. D. & Ryan, P. J. (1980) *Nature 287*, 160–161.
8. Matthew, E., Laskin, J. D., Zimmerman, L., Weinstein, I. B., Hsu, K. C. & Engelhardt, D. L. (1981) *Proc. Natl Acad. Sci USA 78*, 3935–3939.
9. Wang, K. T., Morgan, J. I. & Spector, S. (1984) *Proc. Natl Acad. Sci. USA 81*, 3770–3772.
10. Ishiguro, K., Taft, W. C., Delorenzo, R. J. & Sartorelli, A. C (1987) *J. Cell Physiol. 131*, 226–234.
11. Besman, M. J., Yanagibashi, K., Lee, T. D., Kawamura, M., Hall, P. F. & Shively, J. E. (1989) *Proc. Natl Acad. Sci. USA 86*, 4897–4901.
12. Yanagibashi, K., Ohno, Y., Nakamichi, N., Matsui, T., Hayashida, K., Takamura, M., Yamada, K., Tou, S & Kawamura, M. (1989) *J. Biochem. (Tokyo) 106*, 1026–1029.
13. Mukhin, A. G., Papadopoulos, V., Costa, E. & Krueger, K. E. (1989) *Proc. Natl Acad. Sci. USA 86*, 9813–9816.
14. Sprengel, R., Werner, P., Seeburg, P. H., Mukhin, A. G., Santi, M. R. Grayson, D. R., Guidotti, A. & Krueger, K. E. (1989) *J. Biol. Chem. 264*, 20415–20421.
15. Riond, J., Vita, N., Le Fur, G. & Ferrara, P. (1989) *FEBS Lett. 245*, 238–244.
16. Chasin, L. & Urlab, G. (1980) *Proc. Natl Acad. Sci. USA 77*, 4216–4220.
17. Ferrara, P., Pecceu, F., Marchese, E., Vita, N., Roskam, W. & Lupker, J. (1987) *FEBS Lett. 226*, 47–52.
18. Sundstrom, C. & Nilsson, K. (1976) *Int. J. Cancer 17*, 565–577.

19. Cleveland, D. W., Fischer, S. G., Kirschner, M. W. & Laemmli, U. K. (1977) *J. Biol. Chem. 252*, 1102–1106.
20. Houghten, R. A. (1985) *Proc. Natl Acad. Sci. USA 82*, 5131–5135.
21. Cathala, G., Savouret, J. F., Mendez, B., West, B. L., Karin, M., Martial, J. A. & Baxter, J. D. (1983) *DNA 2*, 329–335.
22. Caput, D., Beutler, B., Hartog, K., Thayer, R., Brown-Shimer, S. & Cerami, A. (1986) *Proc. Natl Acad. Sci. USA 83*, 1670–1674.
23 Sanger, F., Nicklen, S. & Coulson, A. R. (1977) *Proc. Natl Acad. Sci USA 74*, 5463–5467.
24 Mattei, M. G., Philip, N., Passage, E., Moian, J. P., Mandel, J. L. & Mattei, J. F. (1985) *Hum. Genet. 69*, 268–271.
25 Doble, A., Ferris, O., Burgevin, M. C., Menager, J., Uzan, A., Dobroeucq, M. C., Renault, C., Gueremy, C. & Le Fur, G. (1987) *Mol. Pharmacol. 31*, 42–49.
26. Olson, J. M. M., Junck, L., Young, A. B., Penney, J. B. & Mancini, W. R. (1988) *Cancer Res. 48*, 5837–5841.
27. Kaplan, J. C., Aurias, A., Julier, C., Prieur, M., Szajnert, M. F. (1987) *J. Med. Genet. 24*, 65–78.
28. Kaplan, J. C. & Emanuel, B. S. (1989) *Cytogenet. Cell Genet. 51*, 372–383.
29. Snyder, S. H., Verma, A. & Trifletti, R. R. (1987) *FASEB J. 1*, 282–288.
30. McCabe, R. T., Schoenheimer, J A., Skolnick, P., Hauck-Newman, A., Rice, K. C., Reig, J.-A. & Klein, D. C. (1989) *FEBS Lett. 244*, 263–267.
31. Paul, S. M., Kempner, E. S. & Skolnick, P. (1981) *Eur. J. Pharmacol. 76*, 465–466.
32. Doble, A., Benavides, J., Ferris, O., Bertrand, P., Menager, J., Vaucher, N., Burgevin, M. C., Uzan, A., Gueremy, C. & Le Fur, G. (1985) *Eur. J Pharmacol. 119*, 153–167.

mean tumor growth rate of 0.05 cc per day. Our studies strongly suggest that the novel BK antagonist dimers have clinical potential for the treatment of human lung cancers.

**#1565 Dual potentiation of 1-[β-d-arabinofuranosyl]cytosine (ara-C) action by 7-hydroxystaurosporine (UCN-01) and l-*threo*-sphinganine (safingol; SPC-100270).** Jarvis, W.D., Fornari, F.A., Schwartz, G.K., and Grant, S. *Medical College of Virginia, Richmond, VA 23298, Memorial Sloan-Kettering Cancer Center, New York, NY 10021*

The protein kinase C (PKC) isoenzyme family mediates a cytoprotective influence over leukemic cell survival. Pharmacological inhibition of PKC can promote apoptosis directly, but may also enhance the cytotoxicity of other lethal stimuli. The present study characterized modulation of ara-C-related apoptosis by two PKC inhibitors currently in pre-clinical evaluation: the sphingoid base analog safingol (SPC- 100270), which acts at the lipid-sensitive regulatory domains of cPKC and nPKC, and the staurosporine derivative UCN-01, which acts at the catalytic domains of cPKC, nPKC, and aPKC. Acute (6-hr) exposure of HL-60 human promyelocytic leukemia cells to ara-C (10 μM) resulted in extensive double-stranded DNA damage, impaired clonogenicity, and expression of apoptotic morphology. Ara-C action was enhanced by either SPC (750 nM) or UCN (100 nM) singly; in combination, however, SPC and UCN potentiated ara-C action in a clearly supra-additive (i.e., synergistic) fashion. Thus, whereas the apoptotic capacity of ara-C can be augmented by regulatory domain-selective or catalytic site-selective PKC inhibitors, more effective potentiation is obtained in the combined presence of both classes of agents. We conclude that differential isoform selectivity underlies such synergistic interactions between various classes of pharmacological PKC inhibitors, suggesting that simultaneous targeting of multiple PKC subfamilies may offer distinct advantages over single-agent models of chemopotentiation.

**#1566 Synthesis and biological characterization of aza-anthrapyrazole photoaffinity analogues.** Chou, K-M., Engelke, K., Bigelow, J., Hazlehurst, L., Krapcho, P., and Hacker, M. *University of Vermont, Burlington, VT 05405, Vermont Cancer Center, Burlington, VT 05405*

The anthrapyrazoles recently entered clinical trials and appear to have significant activity against breast cancer. Unfortunately, these drugs are cardiotoxic and ineffective in multidrug resistant (MDR) tumor cells. We previously reported on the synthesis and antitumor characteristics of the 9-aza-anthrapyrazoles, their lack of cardiotoxic potential and cross resistance in MDR models. In an attempt to characterize the interactions of our drugs with the MDR protein we have synthesized a series of photoaffinity analogs. These compounds are cytotoxic, cross resistant in MDR expressing tumor cells and are substrates of the MDR pump (inhibited by verapamil). Using fluorescent and confocal microscopy we have clearly demonstrated that regardless of the photoaffinity analog studied, the replacement of a basic amine on the side chain with an amide results in the photoaffinity analogues being localized in the Golgi and endosomes rather than the nucleus as occurs with the parent compound. These results suggest that the analogs will be useful in determining the MDR affinity and MDR binding sites of our drugs and that the chemical state of the side arm terminal amines plays an important role in directing the intracellular distribution of these drugs.

**#1567 2-Deoxyglucose inhibits antitumor drug-induced apoptosis of human monocytic leukemia U937 cells.** Haga, N., Naito, M., Tomida, A., and Tsuruo, T. *Inst. of Mol. & Cell. Biosciences, Univ. of Tokyo, Tokyo, Japan*

Human monocytic leukemia U937 cells undergo apoptosis when cells are treated with antitumor drugs such as etoposide, CPT and MMC, although molecular mechanism of this drug-induced apoptosis is not well understood. We found that 2-deoxyglucose (2DG) inhibited the apoptosis of U937 cells induced by antitumor drugs. U937 apoptosis induced by TNF alpha, however, was not inhibited by 2DG treatment. 2DG did not induce the expression of anti-apoptotic protein, Bcl-2, and stress proteins such as GRP78 in U937 cells. The formation of DNA-topoisomerase II cleavable complex by etoposide in U937 cells was not affected by the treatment with 2DG, suggesting that 2DG did not reduce the initial cellular damages caused by etoposide. However, 2DG inhibited the etoposide-induced activation of CPP32, an ICE-family protease involved in the development of U937 apoptosis. These results suggest that 2DG inhibits apoptotic signal transduction initiated by antitumor drug-induced cellular damage at a point upstream of ICE famliy-protease activation.

**#1568 Deoxyguanosine kinase overexpression in tumor cell lines.** Hapke, D.M., Stegmann, A.P.A., and Mitchell, B.S. *Departments of Pharmacology and Medicine, University of North Carolina, Chapel Hill, NC 27599*

1-β-D-arabinofuranosylguanosine (AraG) is a guanine analog which has significant promise in the clinic. The extent to which this drug is activated by the cytosolic enzyme, 2'-deoxycytidine kinase (dCK) or by the mitochondrial enzyme, 2'-deoxyguanosine kinase (dGK), is not clear. We have recently cloned the gene encoding dGK and have found a strong structural identity between it and the dCK gene. Overexpression of dCK in tumor cells enhances the sensitivity of these cells to a variety of nucleoside analogs including AraG. To determine whether AraG is also activated by dGK, we infected the small cell lung adenocarcinoma cell line H1437 and CEM T-lymphoblasts with the retroviral vector LNPO, containing dGK cDNA with (dGKm) or without (dGKc) the mitochondrial leader sequence. Northern blots demonstrated increased dGK mRNA in both the LNPO-dGKm and LNPO-dGKc infected cells. There was an increase in dGK activity in the cytosol in LNPO-dGKc infected cells, while dGK activity was increased in mitochondrial fractions of LNPO-dGKm infected cells. These data demonstrate that we are able to direct expression of dGK to either the cytosol or mitochondria, allowing us to determine the relative effects of dGK expression on guanine nucleoside analog toxicity to tumor cells.

**#1569 The peripheral-type benzodiazepine receptor in human breast cancer.** Hardwick, M., Kozikowsky, A., and Papadopoulos, V. *Dept. of Cell Biology, GUMC, Washington, D.C., 20007, Dept. of Neurology, GUMC, Washington, D.C., 20007*

The peripheral-type benzodiazepine receptor (PBR) is a ubiquitous 18KDa protein that has been shown to be involved in the regulation of glioma cell proliferation. Using ligand binding assays we have found that the human breast cancer cell line MDA-MB-231 (231), an extremely aggressive cell line, expresses increased binding of the PBR ligand PK11195 (Bmax=7.8pmol/mg prot, $K_D$=6.6nM) relative to the non-aggressive MCF-7 cell line (not detectable). Northern analysis revealed that this difference in PBR expression is reflected at the PBR mRNA level. Pharmacological analysis of 231 PBR suggests that it is distinct to the PBR seen in other human tissues. Furthermore, subcellular localization of using the fluorescent PBR ligand NBD reveals that 231 PBR is localized to the nuclear membrane whereas MCF-7 PBR is localized to the cytoplasm. Partial nucleotide sequencing of both 231 and MCF-7 PBR cDNA, however, shows no differences with the known human PBR cDNA sequence. Cell proliferation assays using the pyrimidine analog 5-bromo-2'deoxyuridine indicates that nM concentrations of PK11195 stimulate 231 cell proliferation. In conclusion, these studies show a strong correlation between the aggressivity of the human breast cancer cell lines studied and the expression of PBR at both the protein and mRNA levels. Pharmacological analysis, subcellular localization, as well as cell proliferation assays indicate the PBR seen in the 231 cell line is distinct from the PBR studied in other human tissues including the non-aggressive human breast cancer cell line MCF-7. The cell proliferation assays further suggest that PBR ligands can regulate the proliferation of human breast cancer cells presumably through PBR.

**#1570 Cure rate linked to circadian tolerability rhythm of vinorelbine in P388 leukemic mice.** Filipski, E., Breillout, F., and Lévi, F. *Lab. Rythmes Biologiques (Univ. Paris XI and ICIG), Hôp. P. Brousse, Villejuif, France, Pierre Fabre Oncologie, 92100 Boulogne, France*

The effect of circadian dosing time on vinorelbine (VRL) tolerability and antitumor efficacy was investigated in 516 female B6D2F1 mice. Mice were synchronized for 3 weeks by alternating 12h of light and 12h of darkness, then inoculated i.p. with P388 leukemia ($10^6$ cells/mouse) and treated 24h later with i.v. VRL at one of six different circadian times: 3, 7, 11, 15, 19 and 23 hours after light onset (HALO). Single doses tested ranged from 20 to 30 mg/kg. A similar VRL toxicity rhythm was observed in healthy and in tumor-bearing mice: lowest and highest mortality rates corresponded to VRL administration at 19 and at 7 HALO respectively. In P388 mice, increasing VRL dose from 20 to 30 mg/kg did not significantly prolong median survival time if injected at 7 HALO (15.5 and 16.5 days, respectively, p=NS), but did so if treatment was applied at 19 HALO (15.5 and 18.5 days, p<0.007). In order to take full advantage of VRL toxicity rhythm, P388-inoculated mice received 3 weekly injections of 20, 24 or 26 mg/kg/day at one of 4 circadian times: 7, 11, 19 and 23 HALO. Cure rate on day 40 was 3-fold greater in mice treated at 19 HALO as compared to 7 HALO (60% vs 20%). In this tumor model survival prolongation and cures were dose-related and significantly improved by vinorelbine dosing at its least toxic time (mid to late activity span).

**#1571 Methylene blue viral photo-inactivation is associated with formation of RNA-protein crosslinks.** Schneider, J.E., Jr., Lin, X-L., Marble, P., Thomas, T., Pye, Q., Tang, J., and Floyd, R.A.

Methylene blue plus light (MB+L) is known to inactivate some viruses very efficiently, and is currently in use as a treatment of blood products in order to inactivate undetected viruses, including the human immunodeficiency virus (HIV-1). MB+L forms 8-hydroxyguanine (8-OHGua) in RNA and DNA and protein crosslinks in the RNA bacteriophage Qβ. RNA-protein crosslinks occur at a rate that makes them a candidate for the primary inactivation lesion(s) in Qβ during MB+L exposure. We show with an infectious RNA assay that Qβ RNA is much more rapidly inactivated by MB+L when it is exposed to the intact virion, as compared to purified RNA. This is interpreted to mean that the association of the phage proteins with the genomic RNA of the phage enhance the inactivation of the RNA. Formally, such enhanced inactivation by the proteins could be due to: 1) RNA-protein crosslink formation; 2) conformational differences in the RNA that make the RNA a more sensitive target for the MB+L reaction; or 3) enhanced photolytic damage to the RNA due to the presence of amino acids in close proximity to the RNA. In contrast with the Qβ phage system, the HIV-1 RNA virus has many proteins in its virion structure, some of which have enzymatic activities. We show that HIV-1 viruses are inactivated by MB+L exposure at a much faster rate than is the reverse transcriptase (RT) associated with the HIV-1 virion. Data

# PROCEEDINGS

## EIGHTY-EIGHTH ANNUAL MEETING




**APRIL 12-16, 1997**
**SAN DIEGO, CA**

**VOLUME 38 ■ MARCH 1997**

# PROCEEDINGS

## 88th Annual Meeting of the American Association for Cancer Research

April 12-16, 1997 • San Diego, CA
VOLUME 38 • MARCH 1997

## CONTENTS


| ABSTRACTS | Page |
|---|---|
| **Biology** | |
| Cell Death: Mechanisms I | 47 |
| Angiogenesis | 51 |
| Cell Death: bcl-2 and CASPASES | 132 |
| Signaling Pathways | 137 |
| Cell Surface, Metastasis, Differentiation | 142 |
| Proteinases: Invasion and Regulation | 165 |
| Cell Death: Genes I | 169 |
| Cell Death: FAS and Drug-induced | 192 |
| Cell Cycle I | 197 |
| Invasion and Angiogenesis: Inhibitors and Suppressor Genes | 202 |
| Angiogenesis | 263 |
| Cell Death: Genes II | 283 |
| Cell Motility and Adhesion | 287 |
| Regulation of Apoptosis | 344 |
| Invasion and Metastasis: MMPS and TIMPS | 405 |
| Invasion and Metastasis: Proteinases | 410 |
| Cell Death | 423 |
| Regulation of Cell Cycle | 438 |
| Kinases | 442 |
| Invasion Models, Detection Markers | 489 |
| Cell Cycle II | 493 |
| Differentiation, Apoptosis, Protein Kinase C | 498 |
| Induction and Inhibition of Angiogenesis | 523 |
| Invasion Regulation: Tumor Host Interactions | 532 |
| Cell Death: Human Cancer | 540 |
| Invasion | 545 |
| Growth Factor Signaling | 550 |
| Cell Death: Mechanisms II | 624 |
| TGFβ | 634 |
| **Carcinogenesis** | |
| DNA Damage and Mutagenesis | 37 |
| Oxygen Radicals and DNA Damage | 77 |
| Genetic/Cytogenetic Alterations in Carcinogenesis | 122 |
| Molecular Mechanisms of Carcinogenesis | 127 |
| Molecular Studies in Clinical Populations | 242 |
| Gene Regulation in Tumor Initiation, Promotion, and Progression | 256 |
| DNA Adducts: Identification and Repair | 332 |
| Metabolism and Activation of Carcinogens | 337 |
| Biomarkers in Human Carcinogenesis and Relevant Animal Models | 352 |
| Growth Factors and Signal Transduction in Carcinogenesis | 372 |
| DNA Adduct Formation and Repair: Mutations and Mutation Spectra | 448 |
| Biomarkers and Risk Assessment | 460 |
| Animal and *in Vitro* Models for Human Carcinogenesis | 464 |
| Molecular Mechanisms in Tumor Promotion and Progression | 580 |
| Transformation, Cell Communication, and Mutagenesis | 585 |
| Biomarkers in Risk Assessment | 618 |
| Molecular Responses to DNA Damage | 637 |
| **Clinical Investigations** | |
| Clinical Investigations | 24 |
| Biological and Clinical Studies in Gynecological Malignancies | 104 |
| Applied Molecular Biology in Breast Cancer | 234 |
| Clinical Relevance of p53 Mutations | 254 |

| Clinical Investigations (cont'd) | Page |
|---|---|
| New and Sensitive Diagnostic Techniques | 266 |
| Clinical Investigations in Hematological Malignancies, Sarcomas, and Melanomas | 323 |
| Molecular Biology and Clinical Studies in Lung Cancer and Head and Neck Cancer | 326 |
| Translational Research in Urological and Other Malignancies | 426 |
| From Biology to the Clinical Management of Breast Cancer | 436 |
| Molecular Biology and Clinical Management of Gastrointestinal Cancers | 517 |
| Applied and Molecular Biology for Diagnosis and Clinical Studies in Urological Malignancies | 525 |
| Central Nervous System Tumors: From Molecular to Clinical Diagnosis | 535 |
| Experimental Diagnosis and Treatment of Breast Cancer | 568 |
| **Endocrinology (Preclinical and Clinical)/Signal Transduction** | |
| Growth Factors and Hormonal Effects on Breast, Prostate, and Other Cancers | 55 |
| Hormonal Regulation of Apoptosis and Other Endocrine Signaling Pathways | 114 |
| Endocrine Regulation of Growth, Differentiation, and Cell Death | 172 |
| Estrogen and Its Interactions with Normal and Transformed Breast Tissue | 293 |
| Novel Pathways in Endocrine Signal Transduction | 434 |
| Vitamin D, Retinoids, and Other Steroid Hormone Effects | 451 |
| Antiestrogens, Androgens, and Hormonal Regulation of Breast and Prostate Cancer | 572 |
| **Epidemiology/Prevention** | |
| Diet, Nutrition, and Cancer | 109 |
| Genetic Susceptibility | 167 |
| Biological and Biochemical Mechanisms in Prevention, Biomarkers, and Intervention | 207 |
| Genetic Polymorphisms in Cancer Risk | 211 |
| Molecular Mechanisms of Chemoprevention | 261 |
| Epidemiology, Genetics, and Risk | 298 |
| Chemoprevention I | 361 |
| Chemoprevention II | 366 |
| Genetics and Susceptibility | 457 |
| Biomarkers and Chemoprevention Studies | 527 |
| Molecular and Biological Studies in Prevention | 577 |
| Biomarkers of Exposure and Risk | 627 |
| **Immunology/Preclinical and Clinical Biological Therapy** | |
| Antibodies, Immunoconjugates, Tumor Antigens | 26 |
| Cytokines, Growth Factors, Costimulation | 32 |
| Antibodies, Immunoconjugates | 83 |
| Immunomodulation and Immunosuppression | 118 |
| Tumor Specific Immunity and Animal Models | 237 |
| Nonspecific Effector Mechanisms and Cytokines | 301 |
| Tumor Antigen Presentation, Costimulation, Normal and Abnormal T-Cell Activation | 345 |
| Tumor Antigens, Animal Models, Immunotherapy | 355 |
| Vaccines, CTL | 396 |
| Immunotherapy of Cancer I | 402 |
| Immunotherapy of Cancer II | 487 |
| Cancer Vaccines | 615 |
| Cytokines, Costimulatory Molecules, Immunopotentiation | 629 |

**Molecular Biology/Biochemistry** — Page

- Membrane Transport and Lipid Metabolism 60
- Signal Transduction; Differentiation 63
- Molecular and Related Studies of Oncogenes and Tumor Suppressor Genes 68
- Oncogenes and Tumor Suppressor Genes: From the Bench to the Clinic 80
- Microsatellite Instability 148
- Control of Gene Expression 152
- Viral Oncogenesis 157
- DNA Methylation/DNA Repair 177
- Control of Gene Expression 183
- BRCA1 and 2 and Other Tumor Suppressors or Oncogenes in Breast and Ovarian Cancer 188
- Novel Tumor Suppressor Genes and New Interactions of Known Tumor Suppressor Genes 252
- p53 Status in Human Tumors and Cells 270
- FHIT, p16, and Other Tumor Suppressors and Oncogenes in Human Cancer 274
- Oncogenes, Tumor Suppressor Genes, and Other Studies in Transgenic Mice and Other Rodent Systems 279
- Regulation of Gene Expression in Signal Transduction 347
- Genome Instability: DNA Damage/Repair, Methylation, Amplification 358
- Gene Amplification/Genomic Instability 414
- Control of Gene Expression/Human Neoplasia 418
- Regulation of Gene Expression 445
- Telomerase I 502
- Telomerase/Genomic Instability 507
- Genomic Instability 512
- Control of Gene Expression 555
- Enzymes; Protein-DNA Interactions 559
- myc, ras, TGFβ, and Other Tumor Suppressors and Oncogenes in Cancer Development 564
- Signal Transduction II 619
- Telomerase II 636

**Pharmacology/Therapeutics (Preclinical and Clinical)**

- Alkylating Agents, Platinum Agents, and Taxanes 1
- Gene Therapy: Vectors and Genes 6
- Gene Therapy 11
- Camptothecins and Other Inhibitors of Topoisomerase I 14
- Inhibitors of Topoisomerase II: Actions, Apoptosis, and Resistance 18
- Topoisomerase Pharmacology 73
- Differentiation Therapy 86
- Apoptosis 90
- Polyamines, Ether Lipids, Signal Transduction Inhibitors, and Antifolates 94
- Novel Nucleoside Analogues; Other Novel Antitumor Agents 99
- Molecular Mechanisms Controlling Sensitivity to Antifolates 161
- Gene Therapy: Gene Replacement and Vectors 175
- Novel Antitumor Agents/Natural Products 216
- Phase I Trials 221
- New DNA- and Microtubule-interactive Agents 224
- New Agents–New Targets 229
- Molecular Mechanisms of Drug Resistance 251
- Modulation of Drug Delivery 258
- Topoisomerase Inhibitors; Pharmacology of New Anticancer Agents 304
- Platinum Complexes and Alkylating Agents 310
- Antisense 315
- Combination Therapy 318
- Human Gene Therapy: Clinical Trials and New Approaches 342
- Inhibitors of Farnesyl Protein Transferase and ras Signaling 349
- Gene Therapy: Drug Sensitivity and Resistance 379
- P-Glycoprotein Mediated Drug Resistance 384
- Clinical Drug Resistance 388
- Multidrug Resistance Protein and Drug-Conjugate Mediated Resistance 391
- Drug Targeting 432

**Pharmacology/Therapeutics (Preclinical and Clinical) (cont'd)** — Page

- Drug Transport Mechanisms Associated with Drug Resistance 439
- Kinases and Phosphatases as Targets for Therapy 469
- Inhibitors of Thymidylate Synthase and Related Compounds 474
- Regulation of Drug Resistant Gene Expression 478
- Novel Mechanisms of Drug Resistance 482
- DNA Repair and Drug Resistance 522
- Taxol Action and Resistance 529
- Modulation of Drug Resistance 590
- Pharmacokinetics, Metabolism, and Toxicology 595
- Pharmacology of Anticancer Agents: *In Vitro* Models and Techniques 601
- Drug Screening and Organ Selective Therapy 606
- New Drugs, Drug Design, and New Mechanisms 609
- Thymidylate Synthase Inhibitors 614
- Cell Biology of Topoisomerases and Their Inhibitors 621
- Signal Transduction: Tyrosine Kinase Inhibitors 632

**Radiobiology/Radiation Oncology**

- Radiation Effects: DNA Repair, Signal Transduction, Response Modifiers 42
- Genetic Determinants of Cellular Response to Radiation 163
- Radiation Effects: Normal and Tumor Tissue Response 246
- Photodynamic Therapy, Hyperthermia, and Other Studies 376
- Stress Response and Radiosensitization 537

**EXTENDED ABSTRACTS**

**Special Lectures**

- Presidential Address 640
- G.H.A. Clowes Memorial Award 640
- Richard and Hinda Rosenthal Foundation Award 641
- Cornelius P. Rhoads Memorial Award 641
- Bruce F. Cain Memorial Award 642
- American Cancer Society Award 642
- Joseph H. Burchenal AACR Clinical Research Award 643

**Symposia**

- Demystifying the Role of Cytokines in Tumor Immunobiology: Status and Future Utility 644
- Epidemiology and Pathogenesis of Secondary Cancers 645
- Animal Models for Functional Analysis of Tumor Suppressor Genes 647
- Cell Cycle Regulation 648
- Gene Interactions with the Environment/Carcinogenesis 650
- Identification and Management of Genetic-High-Risk Individuals 651
- Breast Cancer Genes 653
- Apoptosis and Cancer Therapy 654
- Cellular Responses to Endogenous *versus* Environmentally Induced DNA Damage 655
- Diagnostic, Prognostic, and Therapeutic Aspects of Tumor Suppressor Genes 657
- Signaling Pathways for Novel Therapeutics 658
- Telomerase and Clinical Applications 658
- Metastasis, Invasion, and Angiogenesis: Mechanisms and Therapeutic Strategies 659
- Colon Cancer 663

**AUTHOR INDEX**

- Proffered Papers 666
- Extended Abstracts of Invited Papers 705

**SUBJECT INDEX** 706

**BUSINESS PROCEEDINGS** 796

**EMPLOYMENT REGISTER** 811

**SUSTAINING MEMBERS** 817